Journal of
Translational Medicine

RESEARCH

Check for updates

Survival advantage of native and engineered T cells is acquired by mitochondrial transfer from mesenchymal stem cells

Angela C. Court[1,2,3†], Eliseo Parra-Crisóstomo[2,3†], Pablo Castro-Córdova[1,3†], Luiza Abdo[4], Emmanuel Arthur Albuquerque Aragão[4], Rocío Lorca[1,3], Fernando E. Figueroa[1,3,5], Martín Hernán Bonamino[4,6] and Maroun Khoury[1,2,3,5*]

Abstract

Background Apoptosis, a form of programmed cell death, is critical for the development and homeostasis of the immune system. Chimeric antigen receptor T (CAR-T) cell therapy, approved for hematologic cancers, retains several limitations and challenges associated with ex vivo manipulation, including CAR T-cell susceptibility to apoptosis. Therefore, strategies to improve T-cell survival and persistence are required. Mesenchymal stem/stromal cells (MSCs) exhibit immunoregulatory and tissue-restoring potential. We have previously shown that the transfer of umbilical cord MSC (UC-MSC)-derived mitochondrial (MitoT) prompts the genetic reprogramming of CD3+ T cells towards a T_{reg} cell lineage. The potency of T cells plays an important role in effective immunotherapy, underscoring the need for improving their metabolic fitness. In the present work, we evaluate the effect of MitoT on apoptotis of native T lymphocytes and engineered CAR-T cells.

Methods We used a cell-free approach using artificial MitoT (Mitoception) of UC-MSC derived MT to peripheral blood mononuclear cells (PBMCs) followed by RNA-seq analysis of CD3+ MitoT^{pos} and MitoT^{neg} sorted cells. Target cell apoptosis was induced with Staurosporine (STS), and cell viability was evaluated with Annexin V/7AAD and TUNEL assays. Changes in apoptotic regulators were assessed by flow cytometry, western blot, and qRT-PCR. The effect of MitoT on 19BBz CAR T-cell apoptosis in response to electroporation with a non-viral transposon-based vector was assessed with Annexin V/7AAD.

Results Gene expression related to apoptosis, cell death and/or responses to different stimuli was modified in CD3+ T cells after Mitoception. CD3+MitoT^{pos} cells were resistant to STS-induced apoptosis compared to MitoT^{neg} cells, showing a decreased percentage in apoptotic T cells as well as in TUNEL+ cells. Additionally, MitoT prevented the STS-induced collapse of the mitochondrial membrane potential (MMP) levels, decreased caspase-3 cleavage, increased BCL2 transcript levels and BCL-2-related BARD1 expression in FACS-sorted CD3+ T cells. Furthermore, UC-MSC-derived MitoT reduced both early and late apoptosis in CAR-T cells following electroporation, and exhibited an increasing trend in cytotoxic activity levels.

†Angela C. Court, Eliseo Parra-Crisóstomo and Pablo Castro-Córdova contributed equally to this work.

*Correspondence:
Maroun Khoury
mkhoury@uandes.cl
Full list of author information is available at the end of the article

Conclusions Artificial MitoT prevents STS-induced apoptosis of human CD3$^+$ T cells by interfering with the caspase pathway. Furthermore, we observed that MitoT confers protection to apoptosis induced by electroporation in MitoT^{pos} CAR T-engineered cells, potentially improving their metabolic fitness and resistance to environmental stress. These results widen the physiological perspective of organelle-based therapies in immune conditions while offering potential avenues to enhance CAR-T treatment outcomes where their viability is compromised.

Keywords Mesenchymal stromal/stem cells, Chimeric antigen receptor T (CAR-T) cells, Mitochondria transfer, Induced-apoptosis

Background/introduction

Apoptosis is an evolutionary conserved form of controlled cell death [1]. Either defective or excessive apoptosis is a main contributor to cancer, autoimmunity, or immune deficiency [2]. In the immune system, apoptosis is critical for the development of T and B lymphocytes, ensuring the elimination of self-reactive cells and those unable to recognize the major histocompatibility complex (MHC) before they enter into circulation [3, 4]. Apoptosis also plays a role in activation-induced cell death (AICD) after lymphocyte activation by antigen recognition since it is essential in the contraction phase of the immune response, eliminating activated lymphocytes while preserving the long-lived memory cell population [5]. Different physiological and pathological immune processes stem from increased apoptosis within specific immune cell subsets. Such is the case of acquired immune deficiency syndrome (AIDS), where CD4$^+$ T lymphocytes die due to the infection with the human immunodeficiency virus (HIV-1) or the increased predisposition to undergo apoptosis of CD4$^+$ and CD8$^+$ subsets in old people as a consequence of immunosenescence [6].

On the other hand, CAR-T cells have become of great interest for treating hematological tumors. Recent observations also highlight the potential of CAR-T therapy in other applications including solid tumors, chronic infections, cardiac fibrosis, autoimmune diseases, and cellular senescence [7]. Nevertheless, CAR T-cell therapy retains several limitations, like poor trafficking and tumor infiltration, limited persistence, life-threatening cell-associated toxicities, in addition to the ex vivo manipulation that increases CAR T-cell senescence and susceptibility to apoptosis [8, 9]. CAR-T cells approved or in clinical trials require a viral transfection to provide long-term CAR expression, that holds high production costs and can take up to 15 days to generate the infusion product, while the nonviral transposon-based vector can generate CAR-T cells in 8 days, showing long-term persistence and antitumor response in animal models. However, electroporation with transposon plasmids decreases PBMCs viability to ~20% [10, 11]. Therefore, new therapeutic strategies to overcome these challenges focused on improving T-cell survival are required.

Mesenchymal stem/stromal cells (MSCs), characterized by multipotent and self-renewal capabilities [12], exert anti-inflammatory and immunomodulatory effects through distinct mechanisms such as paracrine signals, including the secretion of soluble factors and extracellular vesicles [13]. MSCs can also exert therapeutic effects by the transfer of functional mitochondria (MitoT) to damaged cells by restoring metabolic and energetic needs [14–16]. We have recently demonstrated that MitoT from umbilical cord (UC)-MSC targets a range of immunocompetent cells, leading to marked changes in immune function. Indeed, MitoT to T CD4$^+$ cells induced a switch toward a functional regulatory T (T$_{reg}$) cell phenotype that curbed the progression of Graft-versus-host disease (GVHD) [17].

Although MitoT is known to rescue damaged cells from several diseases by enhancing their anti-apoptosis ability [18, 19], the effect of MSC-derived MitoT on the survival of apoptotic-challenged native lymphocytes and CAR-T cells has not been addressed. We hypothesized that MitoT could target T-cell apoptosis, regulating cell survival and persistence, two key factors in translational cell therapies.

Metabolic pathways not only provide essential building blocks for unmanipulated T and CAR-T cells during their differentiation and expansion but also significantly influence the outcomes of T-based cell therapy, as recent studies have indicated [20, 21].

To discriminate the level of mitochondria (MT)-dependent immunoregulatory impact without the interference of other mechanisms, here, we used mitoception, which is a cell-free approach using the artificial transfer of isolated MT. Hence, purified UC-MCS-derived MT are incubated with T cells and assayed for MitoT and ensuing functional and metabolic changes. Herein we present evidence supporting the hypothesis that the delivery of UC-MSC-derived MT to human T lymphocytes through the artificial transfer of MT enhances cell survival of native and engineered CAR-T cells (Fig. 1).
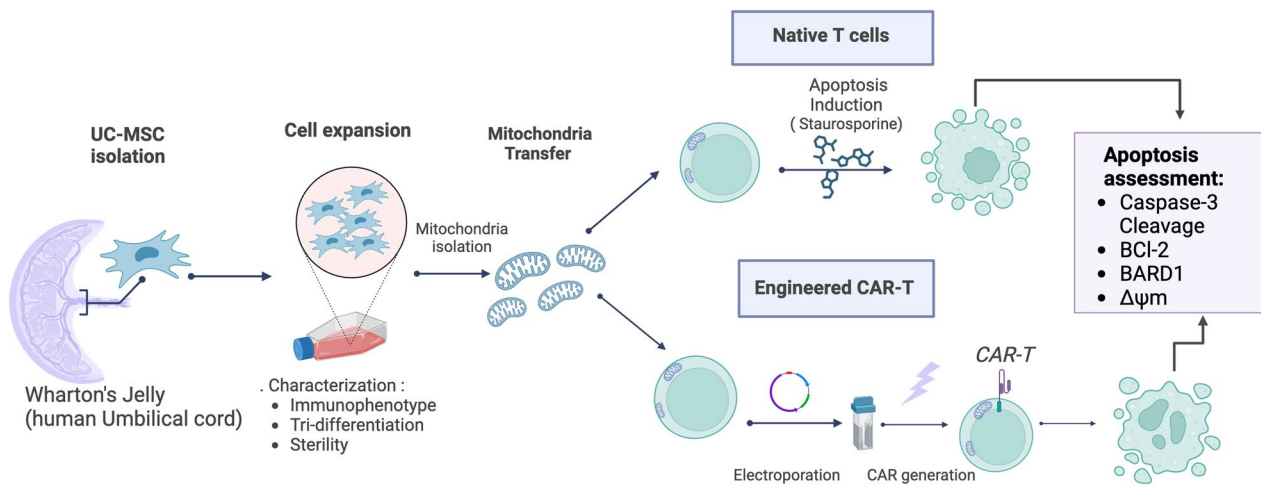
Court *et al. Journal of Translational Medicine*   (2024) 22:868

Page 3 of 15

Fig. 1 Experimental workflow of MitoT to native and CAR engineered T cells. This schematic diagram illustrates the experimental methodology used to isolate mitochondria from umbilical cord MSCs after their transfer into T cells and subsequently challenge them by staurorsporine or through DNA electroporation for CAR-T generation. Apoptosis was then assessed using various markers and membrane potential measurements

Methods

Transcriptome profiling and gene expression analysis.

Whole-genome RNA-Sequencing (RNA-Seq) datasets were downloaded from the Gene Expression Omnibus GSE140483 (SRA numbers SRR10466068–SRR10466075) [17]. Adapter sequences were removed from the raw reads using Trimmomatic version 0.39 [22]. A five-base sliding window quality filtering was also performed, eliminating reads when the average quality of a window fell below $Q < 30$. Reads shorter than 15 nucleotides after trimming were also discarded. The resulting data was mapped to the human genome GRCh38 [23] using HISAT2 version 2.2.1 [24]. Gene expression and differential analysis were performed on annotated genes in the reference genome by using the Transcriptome assembly and differential expression analysis for RNA-Seq platform Cufflinks (http://cufflinks.cbcb.umd.edu/) [25], using the GTF annotation file recovered from the Ensembl database for the human genome GRCh38. Genes were considered as statistically differentially expressed (DE) when presenting an absolute fold change $(FC) > 1.5$ and a p-value < 0.05. Only protein-coding sequences (205 genes) were considered in the following analysis. Volcano plots were created with the analysis results tool CummeRbund following the protocol previously described [25]. Graphical representation of p values versus fold change for the expression datasets was visualized as volcano plot.

Differential gene expression and pathway analysis

We used the web-based Reactome Pathway Database tool (https://reactome.org) and the Cytoscape v.3.9.0 software (https://cytoscape.org) to identify pathways and gene networks that were enriched for DE genes between previously FACS-sorted T CD3^{+} MitoT^{pos} and CD3^{+} MitoT^{neg} cells. Gene Ontology (GO) enrichment was done using the R package "GOfuncR" [26], considering 100 random sets. False Discovery Rate (FDR) multiple testing corrected p-values < 0.05 were used for GO enrichment. Significant DE genes belonging to the GO terms: leukocyte mediated cytotoxicity (GO:0001909), regulation of leukocyte mediated cytotoxicity (GO:0001910), apoptotic process (GO:0006915), defense response (GO:0006952), response to external stimulus (GO:0009605), response to organic substance (GO:0010033), programmed cell death (GO:0012501), regulation of response to external stimulus (GO:0032101), response to chemical (GO:0042221), regulation of apoptotic process (GO:0042981), positive regulation of apoptotic process (GO:0043065), regulation of programmed cell death (GO:0043067), positive regulation of programmed cell death (GO:0043068), regulation of cell differentiation (GO:0045595), lymphocyte activation (GO:0046649), positive regulation of response to stimulus (GO:0048584), negative regulation of response to stimulus (GO:0048585), cellular response to chemical stimulus (GO:0070887), cellular response to organic substance (GO:0071310), cellular response to cytokine stimulus (GO:0071345), were further analyzed.

Cell isolation and culture

Peripheral blood samples were collected from healthy donors with previous informed consent, and Ficoll-Paque Premium density gradient media (GE #17544203) was used for the isolation of PBMCs. For CAR-T experiments, PBMCs were obtained from leukocyte reduction

Court *et al. Journal of Translational Medicine*   (2024) 22:868

Page 4 of 15

filters (RS—Haemonetics) and purified using Ficoll-Paque. Following the general guidelines for the selection of blood donors, the inclusion criteria, included male and female donors, between 25 and 45 years of age, weight more than 50 kg, good level of general health, no anemia or high blood pressure, or any flu symptoms. No chronic diseases, heart disease, or diabetes. The PBMCs were cultured in lymphocyte media (RPMI media supplemented with 10% of FBS, 100 U/mL penicillin, 100 µg/mL streptomycin, 1 mM sodium pyruvate, 1× non-essential amino acids, 2 mM L-glutamine and 25 µM β-mercaptoethanol).

The human UC-MSCs were isolated from healthy donors and characterized according to the International Society for Cell and Gene Therapy (ISCT) minimal criteria, as we previously described [27]. The UC-MSCs used in this present study were plastic-adherent when maintained in standard culture conditions, they express CD73, CD90 and CD105, and lack expression of CD45, CD34, CD14, HLA-DR and CD19 surface molecules, and approved for clinical use [28].

All experiments were performed using early passage (P3–P7) UC-MSCs cultured in humidified incubators at 37 °C with 5% CO_2, using DMEM High Glucose media supplemented with 10% fetal bovine serum (FBS), 2 mM L-glutamine and 100 U/mL penicillin, 100 µg/mL streptomycin. All the procedures presented in this work were approved by the Ethics Committee of Universidad de los Andes, Chile (#CEC202729) and by the Ethics Committee of the Brazilian National Cancer Institute (CEP-INCA)—51589521.4.0000.5274, in conformity with the Helsinki Declaration.

Mitochondria isolation and artificial transfer (Mitoception)
MT in UC-MSCs were labeled with MitoTracker Green FM, MitoTracker Deep Red (500 nM, Invitrogen #M7514; #M22426), or MitoView720 (200 nM, Biotium #70068), and isolated using a commercial kit following the manufacturer's recommendations (ThermoFisher Scientific #89874). Freshly isolated MT from 10^6 to 10^7 UC-MSCs were resuspended in lymphocyte media and transferred to PBMCs in a ratio of 1:10 (MT in quantities equivalent to UC-MSC: PBMC) following the Mitoception protocol [29]. The MitoTracker fluorescence signal stability on $CD3^+$ cells after MitoT was evaluated. (Additional file 1: Figure S1). Immediately, cells were cultured under standard conditions, and after 24 h cells were washed and used for experimental procedures (Fig. 1).

T cell-electroporation
For gene transfer, we used the nonviral transposon-based vector PiggyBac, coding for the 19BBz CAR. 3×10^7 PBMCs were Mitocepted with MitoView720 stained UC-MSC-derived MT in a ratio 1:10 (UC-MSC: PBMC) or as control cells were only cultured with lymphocyte media and were cultured for 24 h at 37 °C, 5% CO_2. Subsequently, mitocepted PBMCs were electroporated in a sterile 0.2 cm cuvette (Mirus Biotech) with the Lonza Nucleofector II electroporation system under the program U-14 with 100 µL of 1SM buffer [30], 10 µg of PBCAG 19BBz (transposon) and 20 µg PBase (transposase), or just with PBase plasmid as control (mock condition). After electroporation, cells were resuspended in 1 mL pf RPMI medium supplemented with 2 mM L-glutamine, 50 U/mL IL-2 (ThermoFisher Scientific #PHC0021), 100 U/mL penicillin, 100 µg/mL streptomycin, 10 mM HEPES, 0.1 mM pyruvate and 20% fetal calf serum and cultured at 37 °C, 5% CO_2. After 2 h, these cells were activated with T Cell TransAct CD3/CD28 (Miltenyi Biotec) at a concentration of 15 µL/mL. On the next day, cell viability was evaluated using Annexin and 7AAD (Fig. 1). The PBCAG GFP transposon plasmid was acquired in Addgene (#40973), and the 19BBz transgene was inserted into the GFP by cloning with restriction enzymes AgeI and NotI. A Myc tag was added to CAR 19BBz between CD8a signal peptide and scFv to allow CAR detection by flow cytometry. The transposase containing plasmid was kindly provided by Dr. Joseph Loturco at the University of Connecticut [31].

Cell viability by Annexin V/7AAD assay
For cell viability and apoptosis assays, 500,000 PBMCs were seeded on a 48-well plate and mitocepted with UC-MSC-derived MT previously labeled with MitoTracker Green at a 1:10 ratio. After 24 h, apoptosis was induced with 10 µM or 20 µM of STS (Abcam #ab120056) for 4 h, as other authors have previously demonstrated protection from apoptosis of human T lymphocytes in vitro [32]. Then, cells were collected and stained with 1:200 anti-CD3-PE (BD #555333) or anti-CD3-PECy7 (BD #557851) antibodies for 30 min at 4 °C protected from light. After washing with PBS, cells were labeled with 1:50 Annexin V-APC (Biolegend #640919) and 1:25 7AAD-PerCP-Cy5.5 (Biolegend #420404) using a commercial binding buffer (Biolegend #422201). For CAR-T experiments, PBMCs were collected and stained with 1:500 anti-CD3-PECy7 (Cytek, #60-0036), 1:100 anti-c-Myc9E10-AlexaFluor647 (Santa Cruz #SC-40), 1:200 Annexin V-FITC (Biolegend #640945), and 1:100 7AAD-PERCP. Data were acquired using FACS Canto II, analyzed with the FlowJo v.10 software, and expressed with the Mean Fluorescence Intensity (MFI) values.

TUNEL assay
Apoptotic cell death was analyzed using the TUNEL assay kit (Abcam, #ab66110) according to manufacturer protocol. Briefly, 500,000 PBMCs were seeded on a

Court *et al. Journal of Translational Medicine*   (2024) 22:868

Page 5 of 15

24-well plate and mitocepted with UC-MSC-derived MT previously labeled with MitoTracker Deep Red at a 1:10 ratio. After 24 h, apoptosis was induced for 4 h with 5 μM or 10 μM STS at 37 °C. Cells were then washed, stained with anti-CD3-PECy7, fixed, and labeled with BrdU-Red and DNA labeling solution, following the manufacturer's recommendations. Finally, cells were collected and analyzed immediately using BD FACS Canto II, and FlowJo v.10 software.

Western blot analysis

Mitocepted PBMCs were seeded on a 6-well plate at a confluence of 1×10^7 cells per well, and 24 h after, apoptosis was induced with 10 μM STS for 5 h. CD3$^+$MitoT^{pos} and CD3$^+$MitoT^{neg} cells were FACS-sorted by using BD FACS Aria Fusion and resuspended with 50 μL of cold Radioimmunoprecipitation Assay (RIPA) buffer containing protease/phosphatase inhibitors (Cell Signaling Technology, #5872). Samples were then sonicated for 5 min at high intensity and centrifuged at 16,000×*g* for 15 min at 4 °C to discard cellular debris. Supernatants were collected, and protein quantification was performed using the Bradford method following the manufacturer's instructions (Bio-Rad, #500-006). 20–30 μg of protein were loaded and electrophoresed into 10% polyacrylamide gels. Next, proteins were transferred to a nitrocellulose membrane and were incubated with a blocking solution (5% Bovine Serum Albumin (BSA) in PBS-Tween 0.01%). Then membranes were incubated with 1:1000 primary antibodies, rabbit anti-Caspase 3, or mouse anti-β-actin (Cell Signaling Technology #9662 and #3700, respectively), and rabbit anti-BRCA1-associated RING domain protein 1 (BARD1) (Novus Biological #NB100-319) and incubated overnight at 4 °C with shaking. Membranes were washed and incubated with 1:20,000 secondary antibodies anti-mouse Alexa fluor 680 (Invitrogen: #A32729) or anti-rabbit Alexa Fluor 800 (Invitrogen #A32735). Finally, membranes were washed, and the fluorescence signal was detected using Odyssey CLx. Analysis was made using Image Studio software (version 5.2).

JC-1 mitochondrial membrane potential assay

To assess the MMP, 500,000 PBMCs were seeded on 48-well plates and mitocepted with UC-MSC-derived MT previously labeled with MitoTracker Deep Red. The next day, cells were treated with 10 μM or 20 μM STS for 5 h to induce apoptosis. Then, cells were collected and stained with anti-CD3 PECy7 antibody for 30 min at 4 °C in darkness, washed once with PBS, and labeled with 2 μM of JC-1 (Invitrogen #M34152) for 30 min at 37 °C and 5% CO_2 conditions. Finally, cells were collected and analyzed immediately using FACS Canto II and FlowJo v.10 software.

RNA extraction and quantitative RT-PCR

For qRT-PCR, total RNA was isolated from 1×10^6 FACS-sorted CD3$^+$ MitoT^{pos} or CD3$^+$ MitoT^{neg} cells, as previously reported [17]. Complementary DNA was prepared in a reverse-transcription reaction using 600 ng of RNA and SuperScript II Reverse Transcriptase (ThermoFisher Scientific #18064014). 5 ng of template mRNA and 5 μM of each forward and reverse human specific primers (Additional file 1: Table S1) were used. qRT-PCR was performed in duplicate on a Stratagene Mx3000P using Brilliant II SYBR Green Master Mix (Agilent Technologies #600828). Data were expressed as relative gene expression using the $2-\Delta Ct$ method and normalized to 18S rRNA housekeeping gene.

Target cell killing assay

To analyze the cytotoxic potential of the generated cells, an in vitro assay was conducted using effector cells against the NALM-6 GFP+ target cells. Prior to the assay, the number of CAR+ cells was verified for all conditions, and the percentage of CAR-T cells was normalized across each donor to ensure uniformity (ranging from 8 to 1% CAR+ cells per donor). The respective donor's Mock (or Mock MitoT^{pos}) was used for this normalization. After 8 days of cell expansion, two different effector-to-target ratios were plated in U-bottom plates: 1:1 (30,000 cells each for effector and target) and 1:2 (15,000 effector cells and 30,000 target cells). Cytotoxicity was assessed at 0 h, 48 h, and 96 h after co-culture by counting the remaining target cells. After each incubation period, the cells were washed and stained with the eBioscience™ Fixable Viability Dye eFluor™ 780 (#65-0865-18), and the samples were analyzed by flow cytometry. To quantify NALM-6 GFP+ cells, dead cells were excluded and the number of GFP+ counts was plotted on a graph to evaluate the lytic potential of the effector cells.

ELISA assay

A co-culture assay was conducted as described in the cytotoxicity assay section. The 1:1 effector-to-target ratio cultivation was performed, and the supernatant was collected 24 h later. The ELISA of IL-2, IFNγ, and TNFα cytokines, the R&D Systems DuoSet kits from catalogs DY202, DY285B, and DY210 were used, respectively. The protocol was followed according to the datasheet specifications, except for the volume reduction in a Corning® 96-Well Half-Area Microplate. In brief, the plate was incubated overnight with 25 μL of the capture antibody solution at the protocol-recommended concentration. Subsequently, 25 μL of the sample's supernatant

Court *et al. Journal of Translational Medicine*   (2024) 22:868

Page 6 of 15

was added and incubated overnight. The next day, the detection antibody and necessary reagents for revelation were added, and all washing and blocking steps were performed as specified. The plate was read on the SpectraMax iD3 at a wavelength range of 450 nm (with 540 nm correction), and quantification in pg/mL was carried out according to the standard curve and blank.

Statistical analysis

In vitro tests were performed using different biological replicates in at least three independent experiments. The data were analysed using GraphPad Prism 10.1.1 software (GraphPad Software, San Diego, CA, USA), and presented as mean ± SEM. Normal distribution was assessed with the Shapiro–Wilk test, and no outliers were removed using ROUT method (Q = 1%). Differences were assessed by two-tailed unpaired Student's t-tests, paired t-test or ANOVA test, as indicated for each figure legends, and considered statistically significant for p values of < 0.05. A heatmap was generated using statistically differentially expressed (DE) genes showing an absolute fold change (FC) > 1.5 and a p-value < 0.05.

Results

Transfer of UC-MSC-derived MT modifies T lymphocyte response to stimulus and apoptosis gene expression

Considering the central role of MT in the control of apoptosis, we assessed whether the direct transfer of active and functional UC-MSCs-derived MT [17, 29] regulates the T cell apoptotic response. We performed whole transcriptome RNA-Seq analysis on previously reported FACS-sorted CD3$^+$ T cells that acquired or not exogenous UC-MSC-derived MT (CD3$^+$ MitoT^{pos} and CD3$^+$ MitoT^{neg} cells, respectively) [17]. Volcano plot analysis derived from FPKM values depicted 205 DE protein-coding genes underexpressed and overexpressed between MitoT^{pos} versus MitoT^{neg} CD3$^+$ cells (Fig. 2A), and pathway enrichment analysis (PEA), using the Reactome tool, revealed the biological functions that were denoted in these genes (Fig. 2B). Among the enriched pathways, GO enrichment analysis revealed 20 gene terms significative enhanced, related to apoptosis, cell death and/or responses to different stimulus in MitoT^{pos} cells (Fig. 2C), and the specific DE genes contained within these GO terms were represented as an unsupervised hierarchical clustering heatmap, showing up or down-regulated transcripts between MitoT^{pos} from MitoT^{neg} CD3$^+$ sorted samples (Fig. 2D).

MitoT from MSC-derived MT grants apoptosis resistance to T cells

To further assess the functional impact of MSC-derived MT on human T-cell apoptotic response, isolated MT

from UC-MSCs were transferred to PBMCs through the mitoception protocol, and 24 h after, the cells were treated with STS, an inhibitor of protein kinase C (PKC), for 4 h to induced apoptosis (Fig. 3A). Cell viability was evaluated by Annexin V/7-AAD assay and flow cytometry gating on CD3$^+$ T population (Fig. 3B). Our results showed that CD3$^+$ MitoT^{pos} cells were significative more resistant to STS-induced apoptosis than MitoT^{neg} cells at either 10 μM or 20 μM of STS (18.4% versus 30.7%, and 26.0% versus 48.0%, respectively; Fig. 3C). Further analysis of apoptotic cell-death by TUNEL staining, corroborated that CD3$^+$ MitoT^{pos} cells were more resistant to STS-induced apoptosis than MitoT^{neg} cells, with a 1.9-fold decrease in the percentage of TUNEL$^+$ cells at 5 μM of STS (Fig. 3D and Additional file 1: Figure S2). Finally, caspase-3 activation was evaluated by western blot by the ratio cleaved caspase 3/pro-caspase 3. We observed that MitoT^{pos} population showed a significative 1.7-fold decrease of cleaved caspase-3 compared with MitoT^{neg} T cells upon STS treatment (Fig. 3E, F), demonstrating the protective role of MitoT from UC-MSCs, preventing the STS-induced apoptosis of CD3$^+$ T lymphocytes.

Since the external MT membrane permeabilization is key in the ongoing downstream apoptosis events, we evaluated the changes in the MMP of T lymphocytes exposed to STS (Fig. 3G). Interestingly, UC-MSC-derived MitoT prevented MT depolarization when comparing MitoT^{pos} and MitoT^{neg} CD3$^+$ T cells after STS treatment (red/green fluorescence ratio of 0.67 versus 0.19 at 10 μM STS (p = 0.009), and 0.60 versus 0.10 at 20 μM STS (p = 0.018); Fig. 3H). These results point to a protective role of MitoT in preventing STS-induced apoptosis by avoiding the dissipation of the MMP.

MitoT increases the expression of anti-apoptotic Bcl-2/BARD1 pathways

To understand the mechanism leading to MitoT-mediated T cell apoptosis resistance, we performed further analysis of the RNA-seq data of the CD3$^+$ MitoT^{pos} and MitoT^{neg} cells. Fold change of the DE genes associated with DNA repair and apoptotic process, regulated after UC-MSC-derived MitoT, revealed that the most differentially upregulated gene was BARD1 (Fig. 4A), involved in the regulation of apoptosis and DNA repair [33, 34]. qRT-PCR analysis confirmed the upregulation of *BARD1* transcript levels in FACS-sorted CD3$^+$ MitoT^{pos}, compared to CD3$^+$ MitoT^{neg} cells (p = 0.052; Fig. 4B). Protein expression levels of full length BARD1 were also significantly increased in MitoT^{pos} sorted CD3$^+$ cells (Fig. 4C), with a 2.1-fold increase (p = 0.033) at 24 h after MitoT (Fig. 4D).

Different anti- and pro-apoptotic proteins belonging to the Bcl-2 family regulate the drop of the MMP

Court *et al. Journal of Translational Medicine*   (2024) 22:868
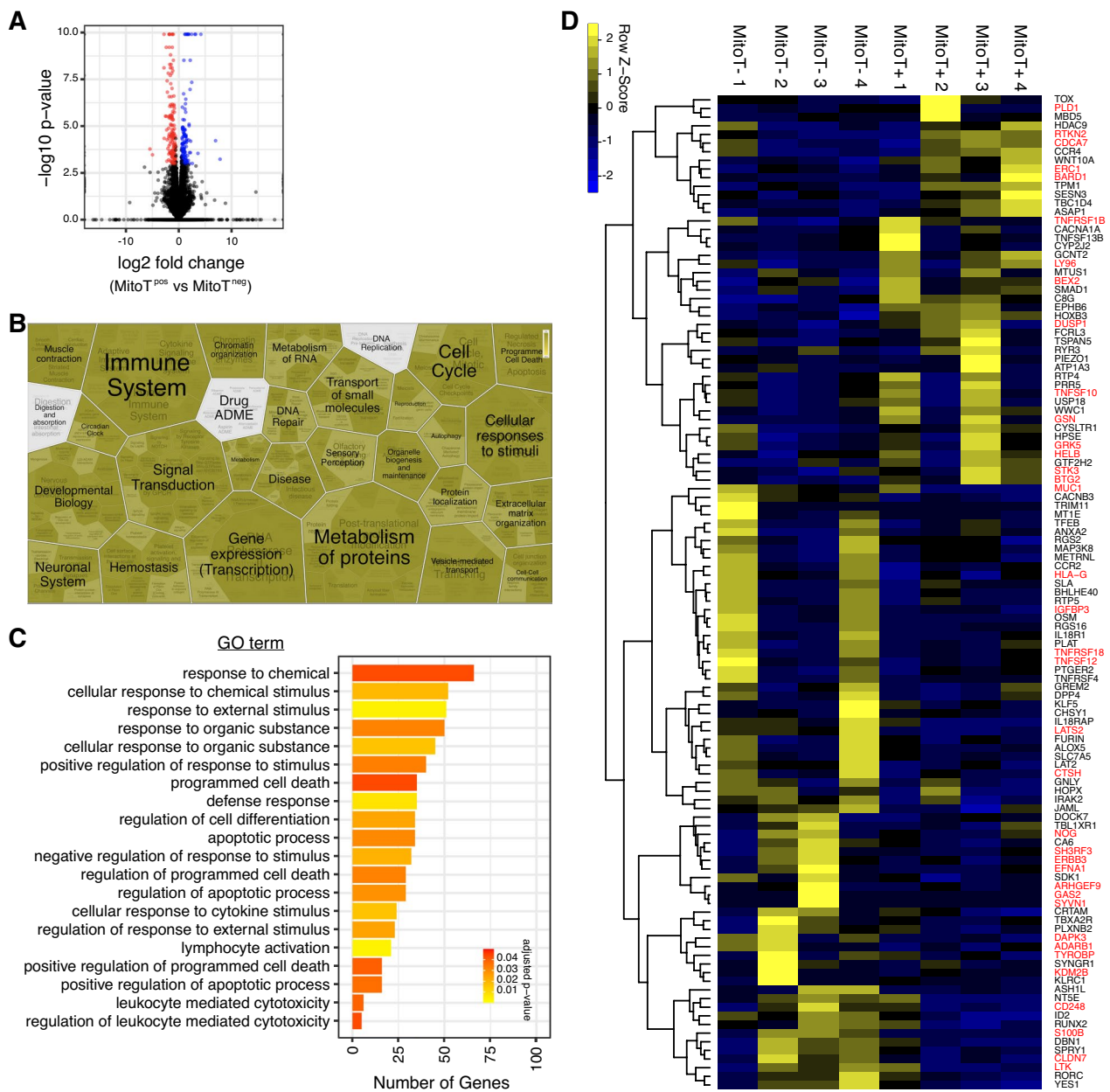
Page 7 of 15

Fig. 2 Transfer of UC-MSC-derived MT modifies T lymphocyte response to stimulus and apoptosis gene expression. **A** Volcano plot analysis derived from FPKM values showing DE genes ($p < 0.05$, Student's t test). Red dots: underexpressed genes (FC MitoT^{pos}/MitoT^{neg} < − 1.5). Blue dots: overexpressed genes (FC MitoT^{pos}/MitoT^{neg} > 1.5). **B** Pathway enrichment analysis (PEA) for DE genes between CD3+ MitoT^{pos} (n = 4) and CD3+ MitoT^{neg} (n = 4) cells. **C** Significantly enriched GO terms related to apoptosis, cell death, and/or responses to different stimuli of DE genes ($p < 0.05$, n = 4) between MitoT^{pos} and MitoT^{neg} cells. **D** Unsupervised hierarchical clustering heatmap of differentially expressed genes associated with GO terms from MitoT^{pos} (n = 4) and MitoT^{neg} (n = 4) samples, from whole transcriptome RNA sequencing analysis. Red transcripts represent genes directly involved in the apoptotic process regulation

and cytochrome c release into the cytosol by inhibiting or inducing the formation of pores on the mitochondrial membrane. Since we observed a preventive effect on the MMP dissipation in MitoT^{pos} T lymphocytes, we further analyzed the Bcl-2 gene network for the DE gene

expression data regulated in MitoT^{pos} CD3$^+$ cells. Using ingenuity pathway analysis, we identify BARD1 and PARK2 transcripts directly related to the Bcl-2 family (Fig. 4E). Finally, qRT-PCR analysis confirmed a significative 7.4-fold increase of *Bcl-2* mRNA transcript levels

Court *et al. Journal of Translational Medicine*   (2024) 22:868
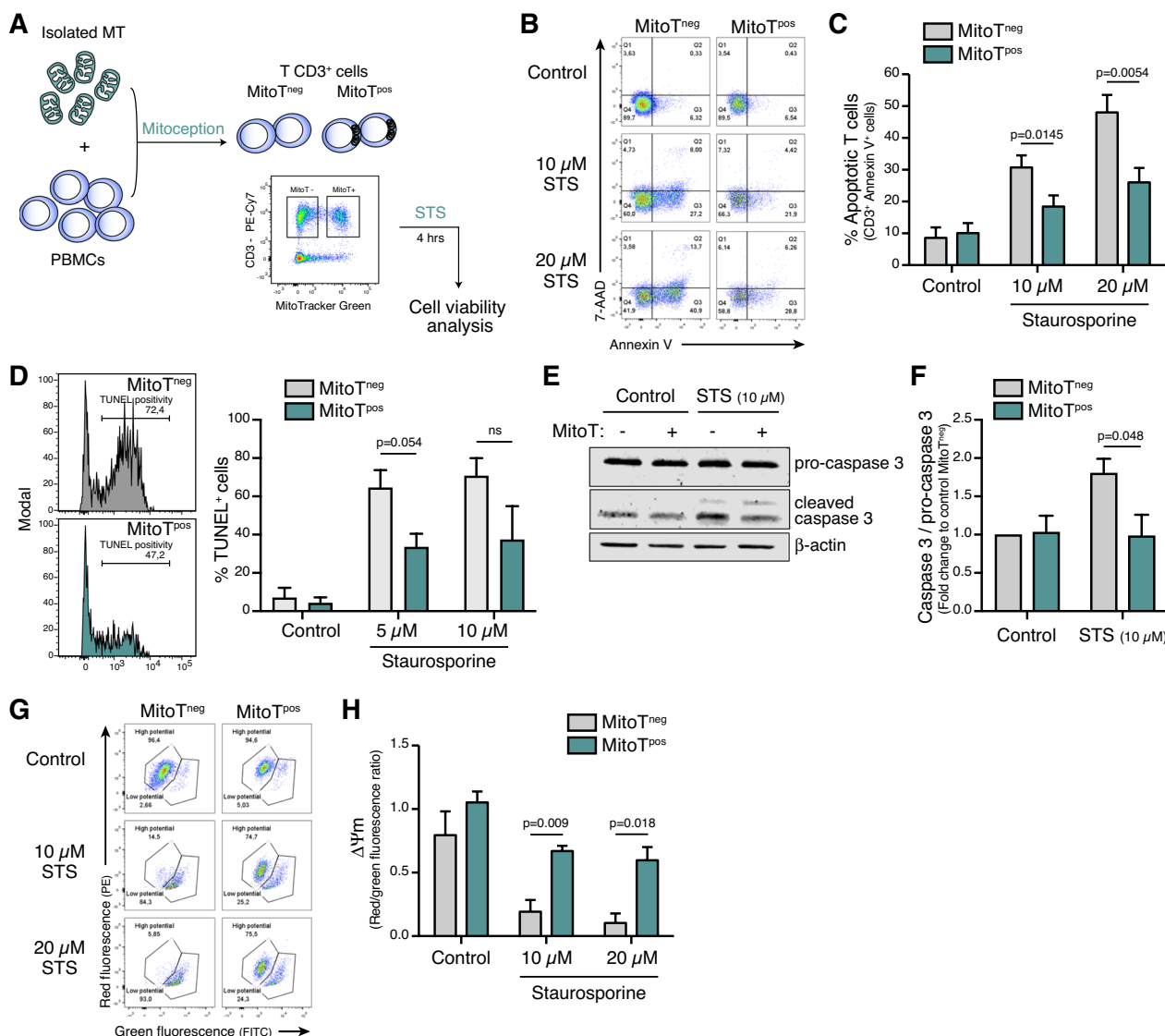
Page 8 of 15

Fig. 3 MitoT from MSC-derived MT grants apoptosis resistance to T cells. **A** Experimental design of artificial MitoT (mitoception) used for apoptosis assays. **B** Representative FACS plots of Annexin V-apoptosis assay on CD3+ MitoT^pos and MitoT^neg populations after 4 h of staurosporine (STS) treatment. **C** Percentage of apoptotic CD3+ MitoT^pos cells compared to MitoT^neg cells after STS treatment. The left bars represented no STS-treatment control (n = 3). **D** Representative TUNEL assay (left panel) and percentage of TUNEL+ cells (right panel), by FACS, of CD3+ MitoT^pos cells compared to MitoT^neg cells after STS treatment (n = 3). **E** Representative western blot of caspase-3 cleavage on MitoT^pos and MitoT^neg CD3+ T lymphocytes after 4 h of STS treatment. β-Actin was used as loading control. **F** Quantification of proteins showed in **E**, represented as caspase 3/pro-caspase-3 ratio in CD3+ MitoT^pos cells compared to MitoT^neg cells (n = 3). **G** Representative FACS plots of the MMP by flow cytometry using JC-1 labeling of T lymphocytes after STS treatment. **H** Mitochondrial depolarization, as the ratio of red to green fluorescence, in CD3+ MitoT^pos cells compared to MitoT^neg cells after STS treatment by FACS analysis (n = 3). For figures **C**, **D**, **F** and **H**: graphs show mean ± SEM and statistical analysis by unpaired t-test. All replicates are biological

in CD3$^+$ MitoT^{pos}, compared to MitoT^{neg} cells (p < 0.05). However, no changes were found in other Bcl-2 family members (Fig. 4F).

Anti-apoptotic effect on CAR-T cells

It has been shown that during CAR-T cell production, especially with the electroporation process, cell viability

decreases ~ 20% [10]. Therefore, since in our experiments MitoT from UC-MSC-derived MT increased apoptosis resistance potential to CD3$^+$ T lymphocytes, we evaluated whether MitoT could protect T cells from apoptosis induced by the electroporation with PiggyBac carrying a c-Myc-tagged version of the 19BBz CAR construct. PBMCs from healthy donors were mitocepted with
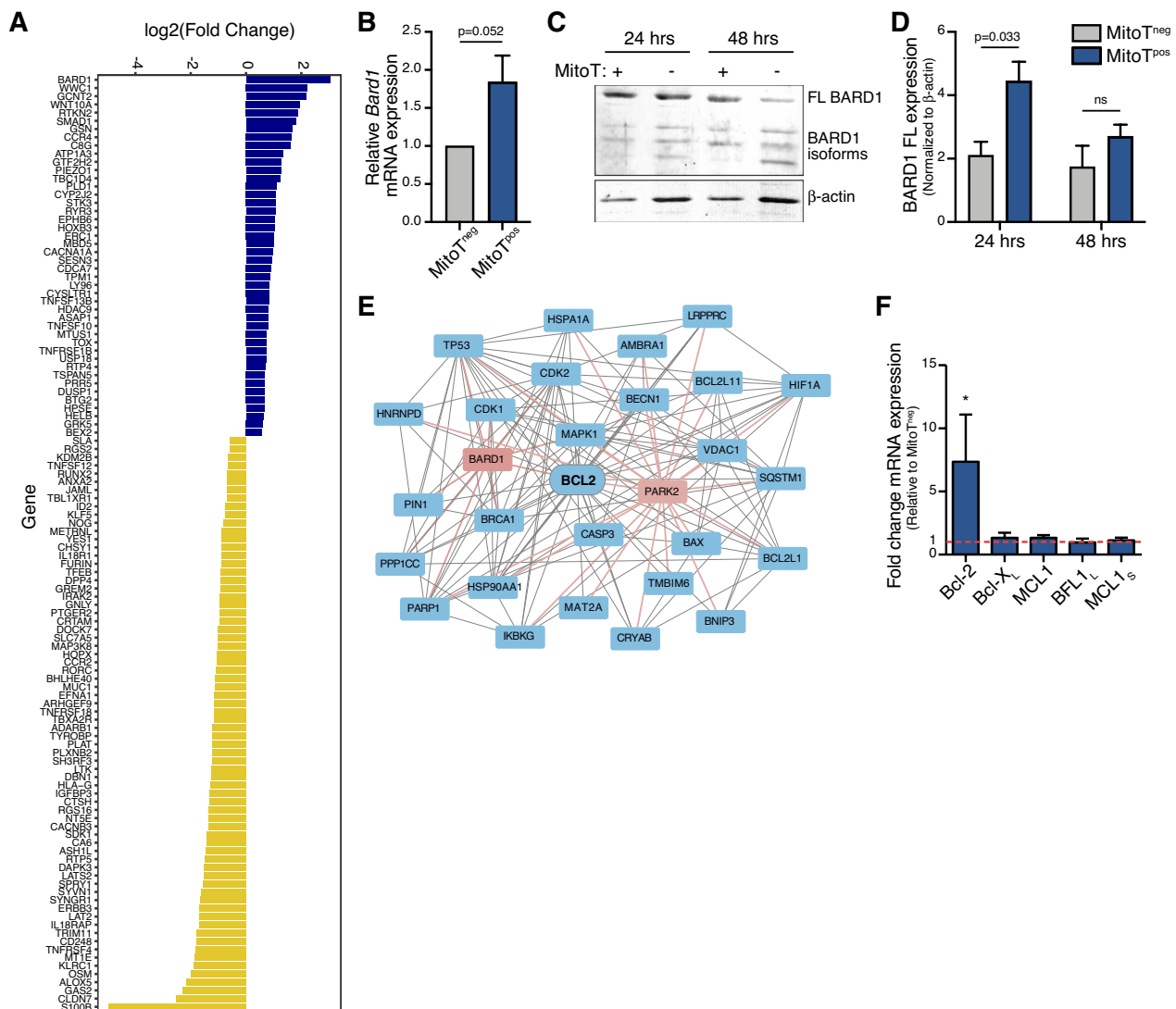
Court *et al. Journal of Translational Medicine*   (2024) 22:868

Page 9 of 15

Fig. 4 MitoT increases the expression of anti-apoptotic Bcl-2/BARD1 pathways. **A** Fold change of differentially expressed (DE) genes contained within the GO terms related to apoptosis, cell death, and/or responses to different stimuli. **B** qRT-PCR analysis of *BARD1* mRNA expression levels in FACS-sorted CD3+ T cells after 24-h post-mitoception with MSC derived-MT (n=4). **C** Representative western blots of BARD1 in FACS-sorted CD3+ MitoT^{pos} cells and MitoT^{neg} cells after 24 or 48 h post-mitoception. **D** Fold change quantification of proteins showed in **C** (n=3). **E** Ingenuity Pathway analysis for Bcl-2 gene network for the DE genes denoted in **A**. **F** qRT-PCR of Bcl-2 family gene expression in FACS-sorted CD3+ MitoT^{pos} cells and MitoT^{neg} cells after 24 h post-mitoception (n=4). For figures **B** and **D**: graphs show mean ± SEM and statistical analysis by unpaired t-test. For figure **F**: graph shows mean ± SEM and statistical analysis by unpaired Mann–Whitney test (*p < 0.05, relative to MitoT[neg] control). All replicates are biological

previously MitoView-labeled MT, electroporated with PiggyBac 19BBz, and cell viability of CAR-T engineered cells was evaluated by Annexin V/7AAD assay (Fig. 5A). We first observed that the transduction efficiency of CAR-T cells was not affected by the MitoT, as a similar percentage of CD3^{+} MitoT^{neg} CAR-T^{pos} and CD3^{+} MitoT^{pos} CAR-T^{pos} cells were found after electroporation (Fig. 5B and Additional file 1: Figure S3A). Interestingly, our results showed that MitoT significantly increased the

cell viability for either CAR-T[neg] (average of 80.1% and 10.2% respectively, p < 0.0001) and CAR-T[pos] (average of 52.2% and 5.6% respectively, p = 0.0053) populations, when comparing MitoT[pos] and MitoT^{neg} cells (Fig. 5C, D). Consistently, we were able to confirm the anti-apoptotic effect of MitoT, since a significant reduction of early and late apoptosis was observed in MitoT[pos] compared to MitoT[neg] subpopulations for both CAR-T[pos] and CAR-T^{neg} cells (Fig. 5C). The results showed a 4.2-fold and

Court *et al. Journal of Translational Medicine*   (2024) 22:868
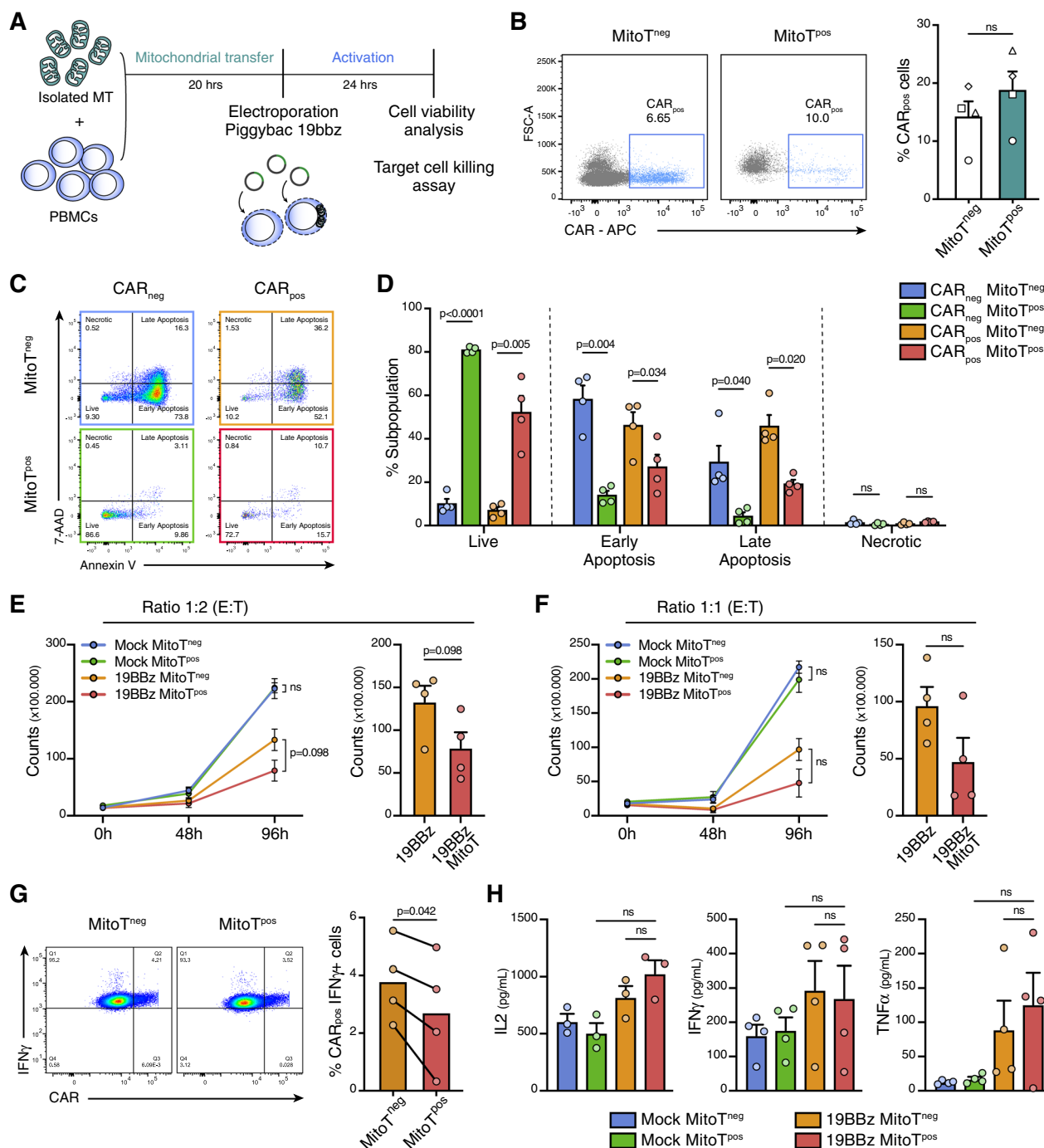
Page 10 of 15

Fig. 5 Anti-apoptotic effect on cMyc-tagged CAR-T cells. **A** Experimental design of artificial MitoT used for apoptosis assay on CAR-T cells. **B** Representative plots (left panel) and percentage of CAR_{pos} cells (right panel), by FACS, of CD3+ MitoT^{pos} cells compared to MitoT^{neg} cells after cell-electroporation (n=4). **C** Representative FACS plots of Annexin V-7AAD apoptosis assay on CD3+ MitoT^{pos} and MitoT^{neg} cells in CAR_{neg} and CAR_{pos} populations after cell-electroporation. **D** Percentage of live, apoptotic, and necrotic CD3+ MitoT^{pos} and MitoT^{neg} cells in CAR_{neg} and CAR_{pos} populations after cell-electroporation (n=4). **E**, **F** Mean of cytotoxicity activity of lymphocytes mitocepted (MitoT^{pos}) or not (MitoT^{neg}) and electroporated with 19BBz or Mock control, against Nalm-6-GFP B-cell line, after 8 days of expansion. The effector cells were incubated in a 1:2 (**E**) or 1:1 (**F**) ratio with the target cells (E:T) for 48 or 96 h. Right bar graph shows the average of remaining target cells (counts) (n=4). **G** Representative plots (left panel) and percentage of CAR_{pos} IFNγ^+ cells (right panel), by FACS, of CD3^+ lymphocytes mitocepted (MitoT^{pos}) or not (MitoT^{neg}) after 8 days of expansion (n=4). **H** Cytokines quantification, by ELISA, on supernatant from lymphocytes expanded and co-cultured for 24 h with target cells (1:1 ratio) (n=4). Graphs show mean±SEM and statistical analysis by unpaired t-test for figures **B** and **D**, paired t-test for figures **E**, **F** and **G**, and One-way ANOVA for figure **H**. All replicates are biological

Court *et al. Journal of Translational Medicine*   (2024) 22:868

Page 11 of 15

17.2-fold reduction of early and late apoptosis in CAR-T_{neg} populations (average of 14% and 1.7% for MitoT^{pos}; and 58.2% and 29.3% for MitoT^{neg}) (p = 0.004 and p = 0.0039, respectively). Similarly, a 1.7-fold decrease and 2.4% reduction of early and late apoptosis were observed in CAR-T_{pos} populations (average of 27.0% and 19.2% for MitoT^{pos}; and 46.2% and 45.9% for MitoT^{neg}) (p = 0.0344 and p = 0.0197, respectively; Fig. 5D). No differences in necrotic subpopulations were observed (Fig. 5C, D). These data showed that MitoT protects CD3$^+$ lymphocytes, especially CD3$^+$ CAR-T engineered cells, from electroporation-induced apoptosis.

Additionally, after CAR-T production by electroporation, the effector function of expanded T cells was evaluated. We observed that 19BBz MitoT^{pos} cells showed an increasing trend in cytotoxic activity against Nalm-6 B cell leukemia after 96 h of co-culture, compared to 19BBz MitoT^{neg} cells, although this difference was not significative (Fig. 5E, F). Curiously, MitoT^{pos} CAR-T_{pos} cells displayed a significantly lower intracellular IFNγ levels than MitoT^{neg} CAR-T_{pos} population (p = 0.042) (Fig. 5G and Additional file 1: Figure S3B, C), but no differences were observed on cytokines released in the supernatant (Fig. 5H and Additional file 1: Figure S3D). Finally, the assessment on exhaustion markers (LAG3, PD1, and TIM3), memory markers (CD95+, CD45RO, and CCR7), and Treg CD4+ expression, showed no differences, neither between the population CD4+CAR+CD4$^+$ CAR-T_{pos} MitoT^{pos} compared to CD4$^+$ CAR-T_{pos} MitoT^{neg}, or between CD4$^+$ CAR-T_{neg} MitoT^{pos} compared to CD4$^+$ CAR-T_{neg} MitoT^{neg} (data not shown).

Discussion

There is growing interest in using MT as a therapeutic agent to treat inflammatory and degenerative diseases. Recent studies revealed that T cells can receive MT from other cell types, affecting T cell development and/ or function. As previously demonstrated by our group, a range of immunocompetent cells, including T and B cells, are receptive for MT of different MSC-sources. Such MitoT has an effect on T cell metabolism, promoting T_{reg} cell differentiation and improvement in tissue damage and survival in a GVHD model of Disease [17]. Similarly, MitoT from MSCs to CD4+ T helper type 17 (Th17) cells promotes metabolic changes, reducing the expression of pro-inflammatory cytokine IL-17 [35], while the transfer of intact MT into rheumatoid arthritis (RA)-associated T cells restores metabolic defects conferring anti-inflammatory properties that reduce disease severity in a humanized mouse model [36]. These data suggest that exogenous MT appear to metabolically reengineer target T cells that might display increased therapeutic potential approach. To this end, it is critically important

to understand the underlying rationale and available evidence that support the use of MT as a cell-free product in ex vivo procedures or in clinical settings.

MT plays a key role in regulating apoptosis in mammalian cells, and its intracellular transfer has been proposed as one of the mechanisms for apoptosis prevention of damaged cells. Indeed, Wang et al. exposed that TNT-mediated transfer of functional MT reversed cellular stress in early apoptotic stages in pheochromocytoma (PC) 12 cells [37]. In a separate approach, the microinjection of intact MT into oocytes reduced their high susceptibility to apoptosis [38].

In the present study, we report that the transfer of isolated active and functional MT from UC-MSCs changes the expression of mRNA transcripts involved in T cell response to stimulus, cell death and apoptosis, including PLD1, BARD1, TNFR2 and DUSP1. We also demonstrated the increase resistance to STS-induced apoptosis in CD3$^+$ T cells that acquired MT from UC-MSCs (CD3$^+$ MitoT^{pos} cells). While these results are consistent with other group reports showing the anti-apoptotic effect of MSCs-derived MT, no study has shown the role of MitoT on the survival of apoptotic-challenged immunocompetent cells. In tenocytes injured by H_2O_2, MitoT rescues distressed cells from apoptosis, and prevents Achilles tendinopathy in vivo [39]. Additional work has shown that the active MitoT from adult MSCs to mtDNA-deficient cells increases survival and restores their MT function [40]. Also, in odontoblasts, bone marrow MSCs (BMSC)-derived MitoT protects from pyroptotic cell death in response to dental pulp damage [41].

The selection of an appropriate tissue source for MSCs used in the isolation of MT requires a balancing of considerations, including cell yield, potency and clinical testing. We have selected the umbilical cord source due to its extensive use in clinical trials, supported by our group's experience with UC-MSCs across various completed clinical applications [28, 42–44].

Preservation of the permeability of the MT outer membrane is crucial for cell survival. It is known that one of the main pathways of apoptosis involves Caspase-3 which, when activated, catalyzes the cleavage of numerous key cellular proteins and changes the MT membrane permeability and swelling [45]. Here, when caspase-3 activation was measured following protein cleavage, CD3$^+$ MitoT^{pos} cells displayed decreased levels of cleaved caspase-3 compared with the MitoT^{neg} population. Additionally, since the decline in MMP and further release of cytochrome c from MT are key events during apoptosis, we assayed the effect of MitoT on MT membrane depolarization in apoptotic-challenged T lymphocytes. We observed that UC-MSC-derived MitoT prevented the reduction of MMP induced by STS in CD3$^+$ MitoT^{pos}

Court *et al. Journal of Translational Medicine*   (2024) 22:868

Page 12 of 15

cells, reinforcing the protective role of MitoT in STS-induced apoptosis. Furthermore, Anti-apoptotic Bcl-2 family members have been shown to inhibit the release of cytochrome c and loss of the MMP associated with apoptosis [46]. Within our experimental setting, an increased expression of the anti-apoptotic gene Bcl-2 was detected in FACS-sorted MitoT^{pos} CD3$^+$ cells, suggesting that the prevention of the drop in the MMP might be mediated by the increase in the Bcl-2 expression.

These results present a new approach to increase the survival advantage of T cells and improve their resistance to environmental stress following their transplantation. For example, Tschumi et al. showed that CAR-T cells progressively upregulate Fas, FasL, DR5, and TRAIL, which result in their programmed cell death independently of their antigen-mediated TCR or CAR activation [47]. Improving the fitness, survival, and persistence of T cells used in immunotherapy has important translational value because they constitute key factors when assessing an effective therapy outcome. As an example, adoptive cell therapy of T_{reg} cells for the treatment of autoimmune diseases also encounters limitations given the ex vivo expansion of T_{reg} cells is patient-dependent. In addition, they require IL-2 infusion to support cell survival and also patients under this treatment are often in need of further immunosuppressant drugs that limit both survival and proliferation of T_{reg} cells [48].

It is noteworthy that the observed protective effect is closely associated with alterations in cellular metabolism, enhanced ATP production, improved cell proliferation, and reduced ROS levels, thereby mitigating mechanical and oxidative stress-induced apoptosis. This may also accelerate metabolic reprogramming, promoting an activated phenotype with increased mitochondrial biogenesis and OXPHOS capacity. This could potentially enhance therapeutic outcomes of CAR-T cell therapy, by improving metabolic fitness and resistance to apoptosis.

Interest in CAR-T therapy has increased exponentially in recent years as clinical applications seem to expand from hematologic cancers [49] to autoimmune refractory disease [50]. Specifically, the ability of MitoT to prevent apoptosis in T lymphocytes and CAR-T cells suggests a potential therapeutic application in enhancing the efficacy and longevity of CAR-T cell therapies. The latest evidence enphasis the significance of T cell metabolism in cancer therapy, underscoring the necessity for metabolic modulation in CAR T cell therapies for an improved clinical outcome [51].

Most CAR-T-cell approved or in clinical trials require a viral transfection to induce a genetic modification, which is associated with high production costs, increased production time, and cumbersome quality controls that are reflected in the final cost of CAR-T therapy. Therefore,

technologies that reduce manufacturing time and costs, while maintaining T-cell function are a requisite to expand the usage of CAR T-cell therapy. New approaches with virus-free and in vivo gene delivery systems offer promising avenues to this effect [52]. Several groups described the use of Sleeping Beauty (SB) transposons for CAR T-cell generation [53, 54]. As shown by Chicaybam et al., efficient genetic modification of T lymphocytes with high and long-term CAR expression was induced with the SB transposon system, displaying antitumor activity in vitro and in vivo [10]. Moreover, the authors also describe a protocol to generate 19BBz CAR-T cells in 8 days, with clinical-grade applications, developed to meet the increasing demand for this therapy [11]. Clinical trials applying electroporation to generate CAR-T cells using non-viral vectors such as Sleeping Beauty or PiggyBac are underway [55–58]. In addition, electroporation results support good clinical results and therapeutic potential for CAR-T cells using this platform [59, 60]. Nevertheless, electroporation-induced apoptosis of T cells is a major limit to the efficacy and broad application on the advantages of producing CAR-T cells with non-viral transfection. In this work, we evidenced that MitoT confers a reduction of early and late apoptosis, as observed for both CAR-T$_{pos}$ and CAR-T$_{neg}$ subpopulations. Although most of the clinical applications with transposons were performed with SB-based transposons, whenever a large cargo of transgene is considered (~ 200 kb versus ~ 10 kb), PiggyBac might be the transposon of choice. In this regard, here we validate the anti-apoptotic effect of MitoT in CAR-T cells electroporated with the non-viral transposon-based vector PiggyBac.

CAR-T therapy has potentially severe and hard-to-manage side effects, such as cytokine release syndrome (CRS), neurotoxicity, and macrophage activation syndrome. IFNγ increases CAR-T cytotoxicity and the antitumoral response. However, higher levels IFNγ are related with CRS and neurotoxicity [61]. A recent study evaluated a strategy of neutralizing IFNγ with the monoclonal antibody emapalumab that mitigates severe toxicity related to CAR-T cell therapy [62]. Our results showed that MitoT reduced the expression of IFNγ, displaying an increasing trend in cytotoxic activity against Nalm-6 cells.

Since the long-term persistence, higher cytotoxicity, with lower side effects of CAR-T cells is one of their advantageous traits, we plan to address the antitumor capacity, persistence, and CRS of MitoT CAR-T in future studies with humanized animal models to confirm that these strategies could lead to improved and more affordable CAR-T cell therapy.

The findings presented in this research broaden the physiological perspective of organelle-based therapies

Court *et al. Journal of Translational Medicine*   (2024) 22:868

Page 13 of 15

in immune conditions where the regulation of apoptosis and cell survival is diminished.

Conclusions

We have described a model for the assessment of the protective effect of MitoT on a variety of cell types while showing an acquired survival advantage in specific T and CAR-T cell populations. Our data suggest UC-MSC-derived MitoT regulates CD3$^+$ T cell apoptosis in a BCL2-BARD1-dependent manner, leading to a marked functional impact on T lymphocyte survival. The transfer of external MT might offer an avenue to potentiate the therapeutic effects of adoptive transfer of unmodified T or virus-free based protocols for generating CAR-T cells.

Abbreviations

MSC	Mesenchymal stem/stromal cell
MitoT	Mitochondrial transfer
MT	Mitochondria
MHC	Major histocompatibility complex
AICD	Activation-induced cell death
AIDS	Acquired immune deficiency syndrome
HIV-1	Human immunodeficiency virus
CAR-T	Chimeric antigen receptor T
UC-MSC	Umbilical cord MSC
PBMC	Peripheral blood mononuclear cells
T$_{reg}$	Regulatory T cells
GVHD	Graft-vs-host disease
RNA-Seq	RNA sequencing
DE	Differentially expressed
GO	Gene ontology
ISCT	International Society for Cell and Gene Therapy
STS	Staurosporine
BARD1	BRCA1-associated RING domain protein 1
MMP	Mitochondrial membrane potential
PEA	Pathway enrichment analysis
SB	Sleeping beauty
IL-2	Interleukin 2
IFNγ	Interferon gamma
TNFα	Tumor necrosis factor alpha

Supplementary Information

The online version contains supplementary material available at https://doi.org/10.1186/s12967-024-05627-4.

Supplementary Material 1.

Author contributions

A.C.C., E.P.-C., P.C-C., F.E.F., and M.K. contributed to the conception of the study and experimental design. A.C.C., E.P.-C., P.C-C., L.A., E.A.A and R.L. performed the experiments and data analysis and participated in the acquisition of data. P.C-C., L.A., E.A.A, and M.H.B carried out the cMyc-tagged CAR-T experiments and data analysis. A.C.C., P.C-C., F.E.F. and M.K. wrote and edited this manuscript.

Availability of data and materials

The dataset(s) supporting the conclusions of this article are included within the article and its additional files.

Declarations

Ethics approval and consent to participate

All the procedures presented in this work were approved by the Ethics Committee of Universidad de los Andes, Chile (#CEC202729) and the Ethics Committee of the Brazilian National Cancer Institute (CEP-INCA)—51589521.4.0000.5274.

Consent for publication

Not applicable.

Competing interests

Maroun Khoury is the CEO and CSO of Cells for Cells and Regenero. Angela Court received stipend from Regenero. The remaining authors declare that the research was conducted in the absence of any commercial or financial relationships that could be construed as a potential conflict of interest.

Author details

[1]IMPACT, Center of Interventional Medicine for Precision and Advanced Cellular Therapy, Santiago, Chile. [2]Cell for Cells, Santiago, Chile. [3]Laboratory of Nano-Regenerative Medicine, Centro de Investigación e Innovación Biomédica (CiiB), Faculty of Medicine, Universidad de los Andes, Av. La Plaza 2501, Las Condes, Santiago, Chile. [4]Cell and Gene Therapy Program, National Cancer Institute (INCA), Rio de Janeiro, Brazil. [5]Consorcio Regenero and R-MATIS, Chilean Consortium for Regenerative Medicine, and Manufacture of Advanced Therapies for Innovative Science, Santiago, Chile. [6]Vice-Presidency of Research and Biological Collections (VPPCB), Oswaldo Cruz Foundation, (FIOCRUZ), Rio de Janeiro, Brazil.

References

1. Taylor RC, Cullen SP, Martin SJ. Apoptosis: controlled demolition at the cellular level. Nat Rev Mol Cell Biol. 2008;9:231–41.
2. Singh R, Letai A, Sarosiek K. Regulation of apoptosis in health and disease: the balancing act of BCL-2 family proteins. Nat Rev Mol Cell Biol. 2019;20:175–93.
3. Opferman JT. Apoptosis in the development of the immune system. Cell Death Differ. 2008;15:234–42.
4. Rathmell JC, Thompson CB. Pathways of apoptosis in lymphocyte development, homeostasis, and disease. Cell. 2002;109(Suppl):S97–107.
5. Simula L, Corrado M, Accordi B, Di Rita A, Nazio F, Antonucci Y, et al. JNK1 and ERK1/2 modulate lymphocyte homeostasis via BIM and DRP1 upon AICD induction. Cell Death Differ. 2020;27:2749–67.
6. Salvioli S, Capri M, Scarcella E, Mangherini S, Faranca I, Volterra V, et al. Age-dependent changes in the susceptibility to apoptosis of peripheral blood CD4+ and CD8+ T lymphocytes with virgin or memory phenotype. Mech Ageing Dev. 2003;124:409–18.
7. Baker DJ, Arany Z, Baur JA, Epstein JA, June CH. CAR T therapy beyond cancer: the evolution of a living drug. Nature. 2023;619:707–15.
8. Kasakovski D, Xu L, Li Y. T cell senescence and CAR-T cell exhaustion in hematological malignancies. J Hematol Oncol. 2018;11:91.
9. Sterner RC, Sterner RM. CAR-T cell therapy: current limitations and potential strategies. Blood Cancer J. 2021;11:69.
10. Chicaybam L, Abdo L, Carneiro M, Peixoto B, Viegas M, De Sousa P, et al. CAR T cells generated using sleeping beauty transposon vectors and

Court *et al. Journal of Translational Medicine*   (2024) 22:868

Page 14 of 15

expanded with an EBV-transformed lymphoblastoid cell line display antitumor activity in vitro and in vivo. Hum Gene Ther. 2019;30:511–22.

11. Chicaybam L, Abdo L, Viegas M, Marques LVC, de Sousa P, Batista-Silva LR, et al. Transposon-mediated generation of CAR-T cells shows efficient anti B-cell leukemia response after ex vivo expansion. Gene Ther. 2020;27:85–95.

12. Uccelli A, Moretta L, Pistoia V. Mesenchymal stem cells in health and disease. Nat Rev Immunol. 2008;8:726–36.

13. Song N, Scholtemeijer M, Shah K. Mesenchymal stem cell immunomodu-lation: mechanisms and therapeutic potential. Trends Pharmacol Sci. 2020;41:653–64.

14. Spees JL, Olson SD, Whitney MJ, Prockop DJ. Mitochondrial transfer between cells can rescue aerobic respiration. Proc Natl Acad Sci. 2006;103:1283–8.

15. Islam MN, Das SR, Emin MT, Wei M, Sun L, Westphalen K, et al. Mitochon-drial transfer from bone-marrow-derived stromal cells to pulmonary alveoli protects against acute lung injury. Nat Med. 2012;18:759–65.

16. Velarde F, Ezquerra S, Delbruyere X, Caicedo A, Hidalgo Y, Khoury M. Mesenchymal stem cell-mediated transfer of mitochondria: mechanisms and functional impact. Cell Mol Life Sci. 2022;79:177.

17. Court AC, Le-Gatt A, Luz-Crawford P, Parra E, Aliaga-Tobar V, Bátiz LF, et al. Mitochondrial transfer from MSCs to T cells induces Treg differentiation and restricts inflammatory response. EMBO Rep. 2020;21: e48052.

18. Yang F, Zhang Y, Liu S, Xiao J, He Y, Shao Z, et al. Tunneling nanotube-mediated mitochondrial transfer rescues nucleus pulposus cells from mitochondrial dysfunction and apoptosis. Oxid Med Cell Longev. 2022;2022:3613319.

19. Liu Z, Sun Y, Qi Z, Cao L, Ding S. Mitochondrial transfer/transplantation: an emerging therapeutic approach for multiple diseases. Cell Biosci. 2022;12:66.

20. Harada S, Hashimoto D, Senjo H, Yoneda K, Zhang Z, Chen X, et al. Intercellular mitochondrial transfer enhances metabolic fitness and anti-tumor effects of CAR T cells. Blood. 2022;140:2356–7.

21. Kawalekar OU, O'Connor RS, Fraietta JA, Guo L, McGettigan SE, Posey AD, et al. Distinct signaling of coreceptors regulates specific metabolism pathways and impacts memory development in CAR T cells. Immunity. 2016;44:712.

22. Bolger AM, Lohse M, Usadel B. Trimmomatic: a flexible trimmer for Illu-mina sequence data. Bioinformatics. 2014;30:2114–20.

23. Hubbard T. The Ensembl genome database project. Nucleic Acids Res. 2002;30:38–41.

24. Kim D, Paggi JM, Park C, Bennett C, Salzberg SL. Graph-based genome alignment and genotyping with HISAT2 and HISAT-genotype. Nat Bio-technol. 2019;37:907–15.

25. Trapnell C, Roberts A, Goff L, Pertea G, Kim D, Kelley DR, et al. Differential gene and transcript expression analysis of RNA-seq experiments with TopHat and Cufflinks. Nat Protoc. 2012;7:562–78.

26. Grote S. Gene ontology enrichment using FUNC. R Packag version 1180. R package. 2022.

27. González PL, Carvajal C, Cuenca J, Alcayaga-Miranda F, Figueroa FE, Bartolucci J, et al. Chorion mesenchymal stem cells show superior differ-entiation, immunosuppressive, and angiogenic potentials in comparison with haploidentical maternal placental cells. Stem Cells Transl Med. 2015;4:1109–21.

28. Bartolucci J, Verdugo FJ, González PL, Larrea RE, Abarzua E, Goset C, et al. Safety and efficacy of the intravenous infusion of umbilical cord mesen-chymal stem cells in patients with heart failure: a phase 1/2 randomized controlled trial (RIMECARD trial [randomized clinical trial of intravenous infusion umbilical cord mesenchymal]). Circ Res. 2017;121:1192–204.

29. Caicedo A, Fritz V, Brondello JM, Ayala M, Dennemont I, Abdellaoui N, et al. MitoCeption as a new tool to assess the effects of mesenchymal stem/stromal cell mitochondria on cancer cell metabolism and function. Sci Rep. 2015;5:9073.

30. Chicaybam L, Barcelos C, Peixoto B, Carneiro M, Limia CG, Redondo P, et al. An efficient electroporation protocol for the genetic modification of mammalian cells. Front Bioeng Biotechnol. 2017;4:99.

31. Chen F, LoTurco J. A method for stable transgenesis of radial glia lineage in rat neocortex by piggyBac mediated transposition. J Neurosci Meth-ods. 2012;207:172–80.

32. Roesslein M, Schibilsky D, Muller L, Goebel U, Schwer C, Humar M, et al. Thiopental protects human T lymphocytes from apoptosis in vitro

via the expression of heat shock protein 70. J Pharmacol Exp Ther. 2008;325:217–25.

33. Tarsounas M, Sung P. The antitumorigenic roles of BRCA1–BARD1 in DNA repair and replication. Nat Rev Mol Cell Biol. 2020;21:284–99.

34. Russi M, Marson D, Fermeglia A, Aulic S, Fermeglia M, Laurini E, et al. The fellowship of the RING: BRCA1, its partner BARD1 and their liaison in DNA repair and cancer. Pharmacol Ther. 2022;232: 108009.

35. Luz-Crawford P, Hernandez J, Djouad F, Luque-Campos N, Caicedo A, Carrère-Kremer S, et al. Mesenchymal stem cell repression of Th17 cells is triggered by mitochondrial transfer. Stem Cell Res Ther. 2019;10:232.

36. Wu B, Zhao TV, Jin K, Hu Z, Abdel MP, Warrington KJ, et al. Mitochondrial aspartate regulates TNF biogenesis and autoimmune tissue inflamma-tion. Nat Immunol. 2021;22:1551–62.

37. Wang X, Gerdes HH. Transfer of mitochondria via tunneling nanotubes rescues apoptotic PC12 cells. Cell Death Differ. 2015;22:1181–91.

38. Perez GI, Acton BM, Jurisicova A, Perkins GA, White A, Brown J, et al. Genetic variance modifies apoptosis susceptibility in mature oocytes via alterations in DNA repair capacity and mitochondrial ultrastructure. Cell Death Differ. 2007;14:524–33.

39. Wei B, Ji M, Lin Y, Wang S, Liu Y, Geng R, et al. Mitochondrial transfer from bone mesenchymal stem cells protects against tendinopathy both in vitro and in vivo. Stem Cell Res Ther. 2023;14:104.

40. Cho YM, Kim JH, Kim M, Park SJ, Koh SH, Ahn HS, et al. Mesenchymal stem cells transfer mitochondria to the cells with virtually no mitochondrial function but not with pathogenic mtDNA mutations. PLoS ONE. 2012;7: e32778.

41. Wang K, Zhou L, Mao H, Liu J, Chen Z, Zhang L. Intercellular mitochon-drial transfer alleviates pyroptosis in dental pulp damage. Cell Prolif. 2023;56: e13442.

42. Matas J, Orrego M, Amenabar D, Infante C, Tapia-Limonchi R, Cadiz MI, et al. Umbilical cord-derived mesenchymal stromal cells (MSCs) for knee osteoarthritis: repeated MSC dosing is superior to a single MSC dose and to hyaluronic acid in a controlled randomized phase I/II trial. Stem Cells Transl Med. 2019;8:215–24.

43. Matas J, García C, Poblete D, Vernal R, Ortloff A, Luque-Campos N, et al. A phase I dose-escalation clinical trial to assess the safety and efficacy of umbilical cord-derived mesenchymal stromal cells in knee osteoarthritis. Stem Cells Transl Med. 2024;13:193–203.

44. Brizuela C, Meza G, Urrejola D, Quezada MA, Concha G, Ramírez V, et al. Cell-based regenerative endodontics for treatment of periapical lesions: a randomized, controlled phase I/II clinical trial. J Dent Res. 2020;99:523–9.

45. Ricci JE, Gottlieb RA, Green DR. Caspase-mediated loss of mitochondrial function and generation of reactive oxygen species during apoptosis. J Cell Biol. 2003;160:65–75.

46. Harris MH, Thompson CB. The role of the Bcl-2 family in the regula-tion of outer mitochondrial membrane permeability. Cell Death Differ. 2000;7:1182–91.

47. Tschumi BO, Dumauthioz N, Marti B, Zhang L, Schneider P, Mach JP, et al. CART cells are prone to Fas- and DR5-mediated cell death. J Immunother Cancer. 2018;6:71.

48. Esensten JH, Muller YD, Bluestone JA, Tang Q. Regulatory T-cell therapy for autoimmune and autoinflammatory diseases: the next frontier. J Allergy Clin Immunol. 2018;142:1710–8.

49. June CH, O'Connor RS, Kawalekar OU, Ghassemi S, Milone MC. CAR T cell immunotherapy for human cancer. Science. 2018;359:1361–5.

50. Ohno R, Nakamura A. Advancing autoimmune rheumatic disease treatment: CAR-T cell therapies—evidence, safety, and future directions. Semin Arthritis Rheum. 2024;67: 152479.

51. Rial Saborido J, Völkl S, Aigner M, Mackensen A, Mougiakakos D. Role of CAR T cell metabolism for therapeutic efficacy. Cancers. 2022;14:5442.

52. Labanieh L, Mackall CL. CAR immune cells: design principles, resistance and the next generation. Nature. 2023;614:635–48.

53. Monjezi R, Miskey C, Gogishvili T, Schleef M, Schmeer M, Einsele H, et al. Enhanced CAR T-cell engineering using non-viral sleeping beauty trans-position from minicircle vectors. Leukemia. 2017;31:186–94.

54. Singh H, Figliola MJ, Dawson MJ, Olivares S, Zhang L, Yang G, et al. Manu-facture of clinical-grade CD19-specific T cells stably expressing chimeric antigen receptor using sleeping beauty system and artificial antigen presenting cells. PLoS ONE. 2013;8: e64138.

55. Prommersberger S, Reiser M, Beckmann J, Danhof S, Amberger M, Quade-Lyssy P, et al. CARAMBA: a first-in-human clinical trial with SLAMF7

CAR-T cells prepared by virus-free sleeping beauty gene transfer to treat multiple myeloma. Gene Ther. 2021;28:560–71.

56. Magnani CF, Gaipa G, Lussana F, Belotti D, Gritti G, Napolitano S, et al. Sleeping beauty—engineered CAR T cells achieve antileukemic activity without severe toxicities. J Clin Invest. 2020;130:6021–33.

57. Kebriaei P, Singh H, Huls MH, Figliola MJ, Bassett R, Olivares S, et al. Phase I trials using sleeping beauty to generate CD19-specific CAR T cells. J Clin Invest. 2016;126:3363–76.

58. Micklethwaite KP, Gowrishankar K, Gloss BS, Li Z, Street JA, Moezzi L, et al. Investigation of product-derived lymphoma following infusion of piggyBac-modified CD19 chimeric antigen receptor T cells. Blood. 2021;138:1391–405.

59. Nishio N, Hanajiri R, Ishikawa Y, Murata M, Taniguchi R, Hamada M, et al. A phase I study of CD19 chimeric antigen receptor-T cells generated by the PiggyBac transposon vector for acute lymphoblastic leukemia. Blood. 2021;138:3831.

60. Zhang Y, Zhang Z, Ding Y, Fang Y, Wang P, Chu W, et al. Phase I clinical trial of EGFR-specific CAR-T cells generated by the piggyBac transposon system in advanced relapsed/refractory non-small cell lung cancer patients. J Cancer Res Clin Oncol. 2021;147:3725–34.

61. Silveira CRF, Corveloni AC, Caruso SR, Macêdo NA, Brussolo NM, Haddad F, et al. Cytokines as an important player in the context of CAR-T cell therapy for cancer: their role in tumor immunomodulation, manufacture, and clinical implications. Front Immunol. 2022;13: 947648.

62. Manni S, Del Bufalo F, Merli P, Silvestris DA, Guercio M, Caruso S, et al. Neutralizing IFNγ improves safety without compromising efficacy of CAR-T cell therapy in B-cell malignancies. Nat Commun. 2023;14:3423.

Publisher's Note